Journal of Applied Mathematics and Physics, 2024, 12, 126-146
https://www.scirp.org/journal/jamp
ISSN Online: 2327-4379
ISSN Print: 2327-4352

Hydromagnetic Squeezing Nanofluid Flow between Two Vertical Plates in Presence of a Chemical Reaction

Benjamin Matur Madit[1*], Jackson K. Kwanza[2], Phineas Roy Kiogora[2]

[1]Department of Mathematics, Pan African University Institute of Basic Sciences, Technology and Innovation, Juja, Kenya
[2]Department of Pure and Applied Mathematics, Jomo Kenyatta University of Agriculture and Technology, Juja, Kenya
Email: *maturmadit2@gmail.com

How to cite this paper: Madit, B.M., Kwanza, J.K. and Kiogora, P.R. (2024) Hydromagnetic Squeezing Nanofluid Flow between Two Vertical Plates in Presence of a Chemical Reaction. *Journal of Applied Mathematics and Physics*, **12**, 126-146.
https://doi.org/10.4236/jamp.2024.121011

Received: November 23, 2023
Accepted: January 23, 2024
Published: January 26, 2024

Abstract

In this study, Hydromagnetic Squeezing Nanofluid flow between two vertical plates in presence of a chemical reaction has been investigated. The governing equations were transformed by similarity transformation and the resulting ordinary differential equations were solved by collocation method. The velocity, temperature, concentration and magnetic induction profiles were determined with help of various flow parameters. The numerical scheme was simulated with aid of MATLAB. The results showed that increasing the squeeze number only boosts velocity and concentration while lowering temperature. Conversely, increasing the Hartmann number, Reynold's magnetic number, Eckert number and Thermal Grashof number generally increases temperature but decreases both velocity and concentration. Chemical reaction rate and Soret number solely elevate concentration while Schmidt number only reduces it. The results of this study will be useful in the fields of oil and gas industry, plastic processing industries, filtration, food processing, lubrication system in machinery, Microfluidics devices for drug delivery and other related fields of nanotechnology.

Keywords

Hydromagnetic, Squeezing Flow, Nanofluid, Variable Magnetic Field, Chemical Reaction

1. Introduction

Squeezing flow characterized by the movement of one or both confining walls of a channel has diverse applications in engineering and science. Examples include lubrication processes, polymer processing and filtration systems. The addition of

nanoparticles to the base fluid, forming a nanofluid can significantly alter the flow's thermal and physical properties leading to enhanced performance in various applications. This review delves into the recent advancements in the study of nanofluid squeezing flow, focusing on its various influencing factors and their impact on heat transfer, velocity profiles, and other relevant parameters.

Several studies have investigated the dynamics of squeezing flow in various contexts. [1] analyzed the effects of Dufour and Soret numbers on the flow behavior under a variable magnetic field. They observed a direct influence of the squeeze Reynold's number on both temperature and concentration profiles. [2] employed numerical simulations to explore squeezing flow problems and found that increasing the squeezing parameter enhances velocity, thermal, and concentration profiles. The concept of nanofluids was introduced by [3], who defined them as fluids containing a dispersion of nanoparticles with dimensions ranging from 1 to 100 nanometers. These nanoparticles significantly enhance the thermal and electrical properties of the base fluid, making nanofluids highly attractive for various heat transfer applications.

Recent research has explored the impacts of various factors on nanofluid squeezing flow, such as magnetic fields, heat generation, and chemical reactions. [4] found that Cu-Al_2O_3/water hybrid nanofluid enhances heat transfer in a horizontal channel with a magnetic field. However, increasing the squeezing parameter or suction strength worsens the heat transfer coefficient. [5] investigated the combined effects of heat generation and magnetic field strength on the bioconvection of an MHD nanofluid flow. They observed that increasing the magnetic field strength decreases the motile microorganism flux rates and velocity profiles but increases the drag stress and the profiles of mobile microorganisms.

Other studies have focused on the influence of inclined magnetic fields, variable thermal conductivity, slip effects, and chemical reactions. [6] reported that nanoparticles enhance heat transfer in water, while an inclined magnetic field and variable thermal conductivity reduce it. [7] investigated the influence of a variable magnetic field on nanofluid heat transfer between parallel plates. They concluded that the observed results can be utilized to enhance temperature, velocity, and concentration in various applications.

Several other factors, such as geometrical effects, suction/injection, and thermal radiation, can significantly impact nanofluid squeezing flow. [8] highlighted the importance of geometrical effects in enhancing heat transfer within heat exchangers. [9] found that suction/injection decreases velocity and temperature, while increasing the magnetic field parameter increases skin friction coefficient. [10] reported that increasing the magnetic field parameter increases skin friction coefficient, Nusselt number, and nanofluid volume fraction. [11] conducted a thermal transport analysis of squeezing hybrid nanofluid flow using the Response Surface Method. Their findings indicated that increasing the nanoparticle volume fraction decreases the boundary layer thickness and enhances the fluid velocity. Conversely, rising values of the Eckert number increase the fluid temperature, while an increasing squeezing factor reduces the magnetic field distri-

bution of the fluids. [12] analyzed the squeezing flow of nanofluid under a magnetic field. They observed that as the plates approach each other (*i.e.* S < 0), the Eckert (Ec) number and the temperature distribution increase for both Cu-water and Cu-kerosene nanofluids. Furthermore, the nanoparticle concentration parameter and the temperature distribution both increase as the plates move apart. [13] studied the impact of an inclined magnetic field on unsteady squeezing flow with suction/injection. Their results demonstrated that the inclination angle significantly affects the velocity and heat transfer in squeezed flows. [14] investigated the unsteady squeezing flow of magnetized nanolubricant between parallel disks with Robin boundary conditions. They concluded that Robin boundary conditions significantly influence the temperature and nanoparticle concentration profiles and that magnetic nanoparticles can be used to manage heat buildup in squeeze films.

The present study contributes to the advancement of knowledge in nanofluid squeezing flow by investigating the hydromagnetic squeezing flow of a nanofluid between two vertical plates in the presence of a chemical reaction. This study offers several novelties such as: 1) Combined effects of squeezing, magnetic field and chemical reaction: Previous studies have primarily focused on individual or paired effects of these factors. This study offers a comprehensive analysis of their combined influence on the flow behavior, providing valuable insights into real-world applications where these factors co-exist, 2) Vertical plate configuration: Unlike most existing studies on horizontal squeezing flow, this study investigates the flow between vertical plates, which presents a different set of challenges and potential applications, 3) Inclusion of chemical reaction: This study incorporates the effect of a chemical reaction on the mass transfer process within the nanofluid, providing a more accurate representation of situations where chemical reactions occur concurrently with squeezing flow.

By addressing these novel aspects, the present study expands the current understanding of nanofluid squeezing flow and paves the way for further research in this field. The insights gained from this study can be valuable for optimizing various engineering processes and designing innovative technologies that utilize nanofluids for enhanced heat and mass transfer.

2. Mathematical Formulation

Considering a squeezing flow of unsteady, incompressible viscous nanofluid flow between two vertical plates with time varied distance at $x = h(t) = L\left(\sqrt{1-at}\right)$. Depending on the value of a, either the plates are squeezed or separated. If $a < 0$, then the two plates are separated implying that the flow is going backward, while $a > 0$, the two plates are squeezed and touches each other at $t = \frac{1}{a}$, implying that the flow is going forward. The time-varied magnetic field is applied at an oblique angle α with magnetic field strength $\boldsymbol{B} = \left(B_m \cos\alpha, B_m \sin\alpha, 0\right)$ in which $B_m = H_0\left(1-at\right)^{-\frac{1}{2}}$ as given by Jahangeer

[15]. At $t \le 0$, the plates are stationary at temperature $T = T_w$ and the concentration $C = C_w$, respectively. At $t > 0$, the moving plate starts moving with velocity $\frac{\mathrm{d}L}{\mathrm{d}t}$, temperature rises to $T = T_\infty$ and concentration $C = C_\infty$ respectively. Since the flow is in two dimensions, then the velocity, temperature, concentration and induced magnetic field are functions of space coordinates (x, y) and time, *t*. Figure 1 is the schematic configuration of the fluid flow in a vertical plates showing the inclined magnetic field and the squeezing motion of one of the plates as seen below.

3. Governing Equations

The governing equations for this study are in two dimensions given as follow:

Continuity equation

$$\frac{\partial u}{\partial x} + \frac{\partial v}{\partial y} = 0 \tag{1}$$

Momentum equations

$$\rho_{nf}\left[\frac{\partial u}{\partial t} + u\frac{\partial u}{\partial x} + v\frac{\partial u}{\partial y}\right] = -\frac{\partial p}{\partial x} + \mu_{nf}\left[\frac{\partial^2 u}{\partial x^2} + \frac{\partial^2 u}{\partial y^2}\right] + \beta_t \rho g\left(T - T_\infty\right) + \beta_c \rho g\left(C - C_\infty\right) + \sigma\mu_e^2 v\left(B_m \cos\alpha + H_x\right)^2 \tag{2}$$

$$\rho_{nf}\left[\frac{\partial v}{\partial t} + u\frac{\partial v}{\partial x} + v\frac{\partial v}{\partial y}\right] = -\frac{\partial p}{\partial y} + \mu_{nf}\left[\frac{\partial^2 v}{\partial x^2} + \frac{\partial^2 v}{\partial y^2}\right] + \beta_t \rho g\left(T - T_\infty\right) + \beta_c \rho g\left(C - C_\infty\right) + \sigma\mu_e^2 v\left(B_m \cos\alpha + H_x\right)^2 \tag{3}$$

Energy equation

$$\frac{\partial T}{\partial t} + u\frac{\partial T}{\partial x} + v\frac{\partial T}{\partial y} = \frac{K}{\rho_{nf} c_p}\left(\frac{\partial^2 T}{\partial x^2} + \frac{\partial^2 T}{\partial y^2}\right) + \frac{2\mu}{\rho_{nf} c_p}\left[\left(\frac{\partial u}{\partial x}\right)^2 + \left(\frac{\partial v}{\partial x}\right)^2\right] + \frac{\mu}{\sigma_{nf} cp}\left(\frac{\partial u}{\partial y} + \frac{\partial v}{\partial x}\right)^2 + \frac{\sigma\mu_e^2 v^2\left(B_m \cos\alpha + H_x\right)^2}{\rho_{nf} c_p} \tag{4}$$

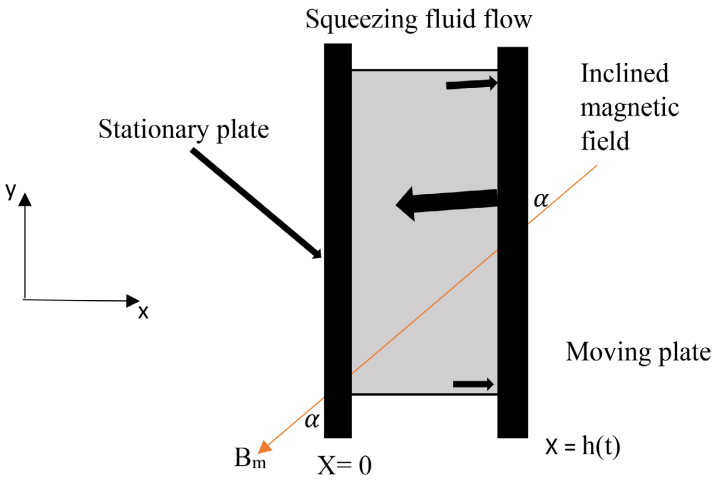

Figure 1. Configuration of the fluid flow.

Concentration equation

$$\frac{\partial C}{\partial t} = -\left[u\frac{\partial C}{\partial x} + v\frac{\partial C}{\partial y}\right] + D_{nf}\left[\frac{\partial^2 C}{\partial x^2} + \frac{\partial^2 C}{\partial y^2}\right] + \frac{D_m K_t}{T_m}\frac{\partial^2 T}{\partial x^2} - k_r\left(C_w - C_\infty\right) \quad (5)$$

Magnetic induction equations

$$\frac{\partial H_x}{\partial t} = H_0\cos\alpha\frac{\partial v}{\partial y} + H_x\frac{\partial v}{\partial y} + v\frac{\partial H_x}{\partial y} + \frac{1}{\mu_e\sigma}\left(\frac{\partial^2 H_x}{\partial x^2} + \frac{\partial^2 H_x}{\partial y^2}\right) \quad (6)$$

$$\frac{\partial H_y}{\partial t} = -\left(H_0\cos\alpha\right)\frac{\partial v}{\partial x} - v\frac{\partial H_x}{\partial x} - H_x\frac{\partial v}{\partial x} + \frac{1}{\mu_e\sigma}\left(\frac{\partial^2 H_y}{\partial x^2} + \frac{\partial^2 H_y}{\partial y^2}\right) \quad (7)$$

These governing equations were transformed using the similarity transformation as stated below.

Similarity transformation

Similarity transformation transforms partial differential equations into ordinary differential equations. The transformations include the following:

$u = -\frac{aL}{\sqrt{1-at}}f(\eta)$, $v = \frac{ay}{1-at}f'(\eta)$, $\theta(\eta) = \frac{T-T_\infty}{T_w-T_\infty}$, $\phi(\eta) = \frac{C-C_\infty}{C_w-C_\infty}$,

$H_x = -\frac{H_0}{\sqrt{1-at}}H(\eta)$, $H_y = \frac{H_0}{1-at}H'(\eta)$, $B_m = H_0(1-at)^{-\frac{1}{2}}$ and $\eta(x,t)$

where $\eta = \frac{x}{L\sqrt{1-at}}$.

Boundary conditions

At $x=0$: $u=0$, $v=0$, $H_x = H_y = 0$, $T = T_w$, $C = C_w$, stationary plate,

At *x*: $x = h(t)$, $u = \frac{\mathrm{d}h}{\mathrm{d}t} = -\frac{aL}{\sqrt{1-at}}$, $v=0$ $H_x = \frac{H_0}{aL}\frac{\mathrm{d}h}{\mathrm{d}t} = -\frac{H_0}{\sqrt{1-at}}$,

$H_y = \frac{H_0}{1-at}$, $T = T_\infty$, $C = C_\infty$, moving plate.

4. Method of Solution

The model equations are solved numerically using collocation method, which is a numerical technique for approximating solutions to various mathematical problems using polynomials. Collocation method has an advantage over other numerical techniques since it provides a continuous approximation to the solution while other numerical techniques approximate solution at a discrete point. Collocation method uses solvers that takes low computational memory and has been tested for the three properties of convergence, consistency and stability by Hale [16]. After converting non-linear Partial Differential Equations (PDEs) to non-linear Ordinary Differential Equations (ODEs) through a similarity transformation, the higher order ODEs are then reduced to a system of first order ODEs. The built-in bvp4c MATLAB function, which provides an approximation based on 4th order, is then used to solve the resulting system of first order ordinary differential equations.

The resulting system of first order ODEs is

$$y_1' = y_2 \quad (8)$$

$$y_2' = y_3 \tag{9}$$

$$y_3' = -S\left[-Sy_1\left(y_1y_2 - \frac{\eta}{2}y_2 - \frac{1}{2}y_1\right) - y_2 - \frac{\eta}{2}y_2 - y_2^2\right] + \frac{S\delta^4}{F_r^2\eta^4} - \frac{Gr\delta^4}{\eta^4}y_4 - \frac{Gc\delta^4}{\eta^4}y_6 - Ha\left[\cos\alpha - y_8\right]^2 y_2 \tag{10}$$

$$y_4' = y_5 \tag{11}$$

$$y_5' = -SPr\left(y_5 - \frac{\eta}{2}y_5\right) - \frac{4PrEc\eta^2}{\delta^2}y_2^2 - \frac{PrEc\eta^4}{\delta^4}y_3^2 - \frac{RPr\eta^4}{\delta^4}\left[\cos\alpha - y_8\right]^2 y_2^2 \tag{12}$$

$$y_6' = y_7 \tag{13}$$

$$y_7' = -Sr\left[-SPr\left(y_5 - \frac{\eta}{2}y_5\right) - \frac{4PrEc\eta^2}{\delta^2}y_2^2 - \frac{PrEc\eta^4}{\delta^4}y_3^2 - \frac{RPr\eta^4}{\delta^4}\left[\cos\alpha - y_8\right]^2 y_2^2 - \right]Sc\left(1 - \frac{\eta}{2}\right)y_7 - \frac{\gamma\delta^2}{\eta^2}y_6 \tag{14}$$

$$y_8' = y_9 \tag{15}$$

$$y_9' = y_{10} \tag{16}$$

$$y_{10}' = -R_m\left[y_8y_3 + y_2y_9 - y_9 + \frac{1}{2}\left(y_8y_2 - \frac{\eta}{2}y_9 - \frac{1}{2}y_8 - \frac{\delta}{\eta}y_2\cos\alpha\right) - \frac{\delta}{\eta}y_3\cos\alpha\right] \tag{17}$$

Subject to the boundary conditions

$$\begin{aligned}&\text{At } \eta = 0: y_1(\eta) = 0, y_2(\eta) = 0, y_8(\eta) = 0, y_9(\eta) = 0, y_4(\eta) = 1, y_6(\eta) = 1\\ &\text{At } \eta = 1: y_1(\eta) = 1, y_2(\eta) = 0, y_8(\eta) = 1, y_9(\eta) = 1, y_4(\eta) = 0, y_6(\eta) = 0\end{aligned} \tag{18}$$

In general, the system takes the form

$$\frac{\mathrm{d}Y}{\mathrm{d}\eta} = f(\eta, Y)$$

where

$$Y = \begin{bmatrix} y_1 \\ y_2 \\ y_3 \\ \vdots \\ y_{10} \end{bmatrix}$$

The system is implemented in MATLAB software using bvp4c built-in function for solving boundary value problems to obtain the profiles of the flow variables.

5. Results and Discussion

The profiles for velocity, temperature, concentration and induced magnetic field

have been determined with help of dimensionless parameters that governed the flow problem and were presented graphically. Parameters such as squeeze number, Hartmann number, chemical reaction rate parameter, Joule heating number, Reynold's magnetic number, Eckert number, Thermal Grashof number, Schmidt number and Soret number were varied to investigate their effects on the flow variables as shown in the figures below.

From Figure 2, it is observed that velocity profiles increase as squeeze number increases. An increase in squeeze number decreases the viscosity in the fluid and the distance between the two plates. This process of squeezing causes the fluid to move faster. As a result, velocity of the fluid increases.

From Figure 3, it is observed that velocity profiles decreases with increase in Hartmann number. The Hartmann number characterizes the strength of the Lorentz force relative to the viscous force. When a magnetic field is applied to an electrically conducting fluid, the Lorentz force acts against the fluid flow, slowing it down. Hence, a higher Hartmann number indicates a stronger magnetic field, which results in a greater reduction in velocity.

From Figure 4, it is observed that velocity profiles decreases with increase in Thermal Grashof number. This is due to buoyancy force which drives a free convection. This force is proportional to the product of the temperature difference, the density difference and the gravitational acceleration. When Grashof number increases, buoyancy force also increases. This causes fluid near the hot surface to rise and the fluid near the cold surface to sink. This creates a velocity gradient in the fluid, with highest velocity develops near the hot surface and the lowest velocity develops near the cold surface. This velocity gradient is responsible for the decrease of the overall velocity of the fluid.

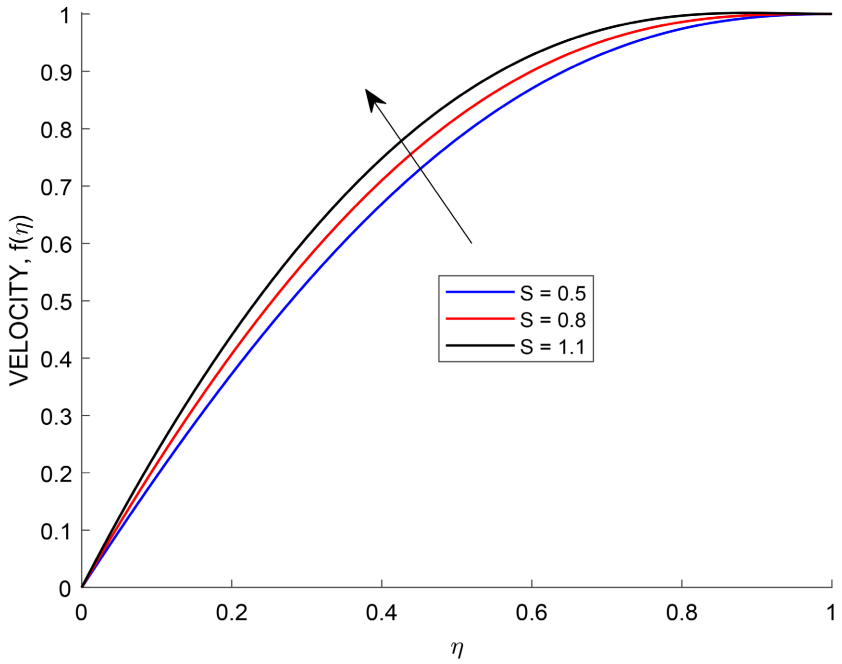

Figure 2. Velocity profiles with varying squeezing number.

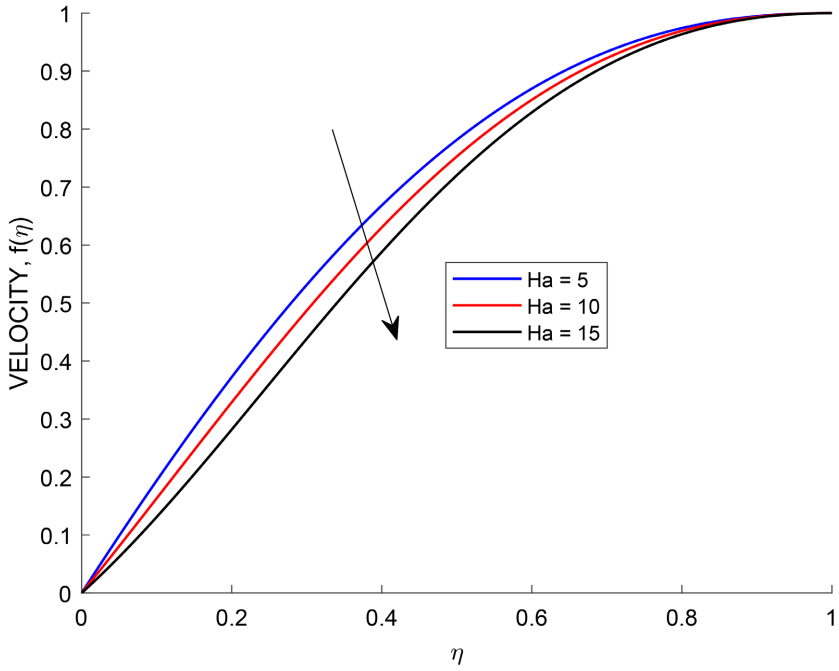

Figure 3. Velocity profiles with varying Hartmann number.

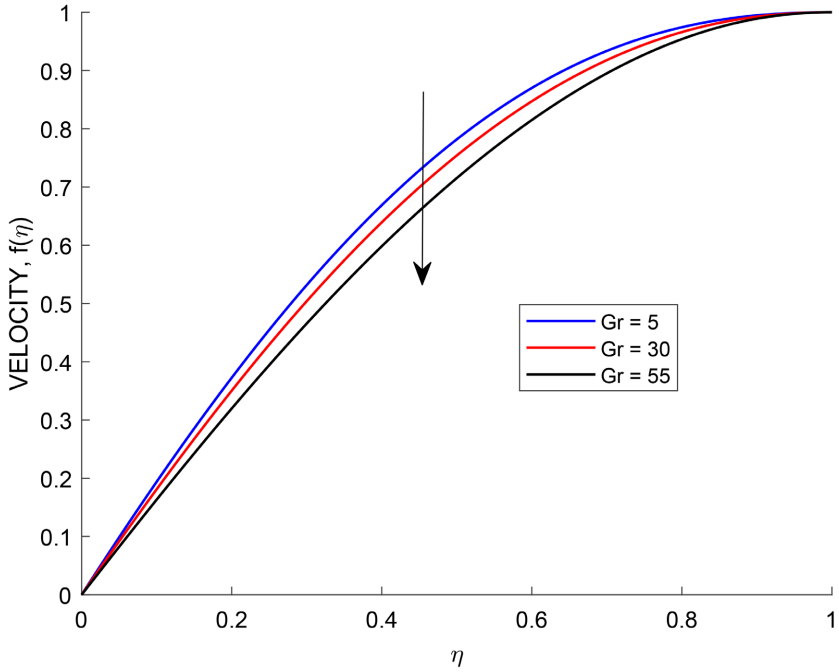

Figure 4. Velocity profiles with varying Thermal Grashof number.

From **Figure 5**, it is observed that temperature profiles decrease with increase in squeeze number. As the fluid is squeezed or compressed between the two surfaces, there is loss of thermal energy in the fluid due to viscous dissipation leading to a decrease in temperature. Secondly, squeezing a fluid can alter its flow patterns and these changes in flow can affect the distribution of temperature as increased flow rate in the squeezed region can lead to mixing of the fluid with

different temperatures which may result in the overall decrease in temperature.

From Figure 6, it is observed that temperature profiles increase with increase in Hartmann number. When the Hartmann number is increased, the Lorentz force increases. This force opposes the flow of the fluid, which causes the fluid to slow down. The low velocity allows the fluid to have more time to absorb heat from the surrounding surfaces. As a result, the temperature of the fluid increases.

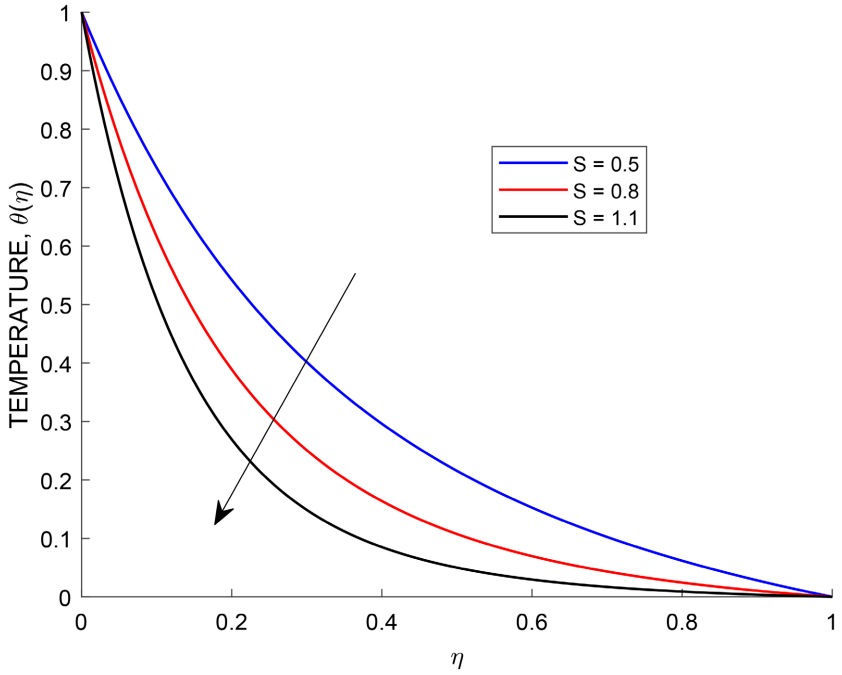

Figure 5. Temperature profiles with varying squeezing number.

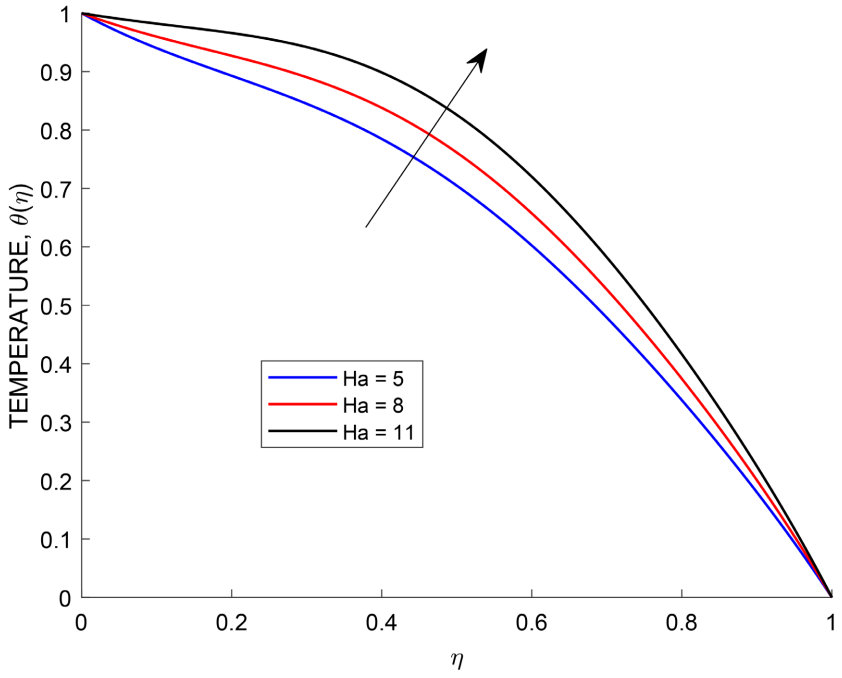

Figure 6. Temperature profiles with varying Hartmann number.

In other words, increase in Hatmann number reduces the magnitude of velocity in the boundary layer, here the temperature in the boundary layer wound increase. Hence, causing the corresponding increase in temperature in the fluid.

From Figure 7, it is observed that temperature profiles increases with an increase in Joule heating. An increase in the Joule heating number results in an increase in the amount of heat generated in the system. This heat is then transferred to the surrounding fluid, which causes the temperature of the fluid to increase.

From Figure 8, it is observed that temperature profiles increase as Reynold's magnetic number increases. Since Reynold's magnetic number increases boundary layer thickness due to lorentz force that acts on the free electrons in the fluid, this has the effect of slowing down the fluid flow and generates heat which increases temperature in the fluid. However, the higher the Reynold's magnetic number, the higher the current that flows through the fluid through the process known as magnetic diffusion and hence more Joule heating occurs and increases temperature in the fluid.

From Figure 9, it is observed that temperature profiles increase with an increase in Eckert number. Eckert number is the ratio of fluid's kinetic energy to thermal internal energy. This is because increase it causes the transformation of kinetic energy into internal energy by work done against the viscous forces in fluid. This enhances heat transfer in fluid which results into an increase in temperature.

From Figure 10, it observed that temperature profiles increases with increase in Thermal Grashof number. An increase in Grashof number means increase in buoyancy force which causes thermal boundary layer thickness to increase which

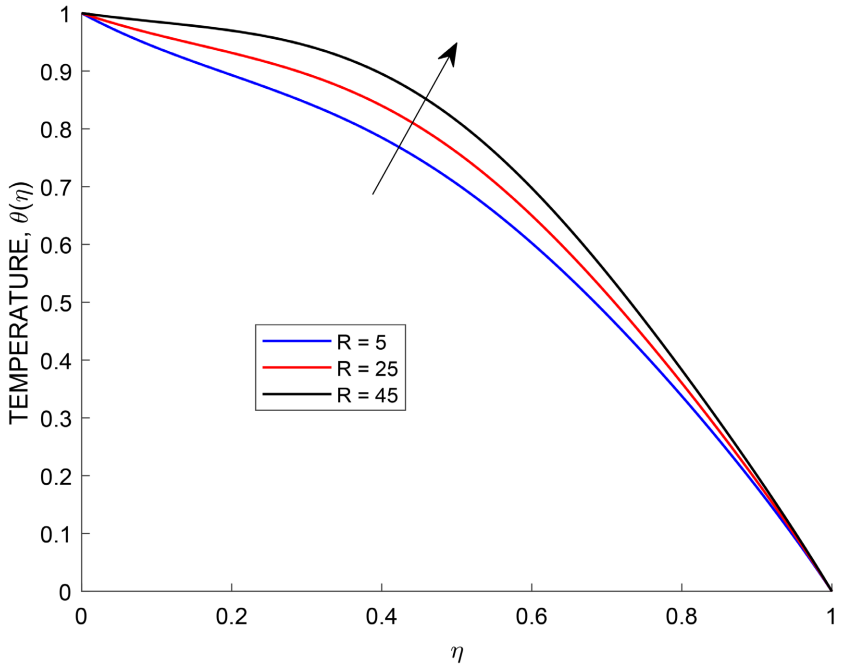

Figure 7. Temperature profiles with varying Joule heating number.

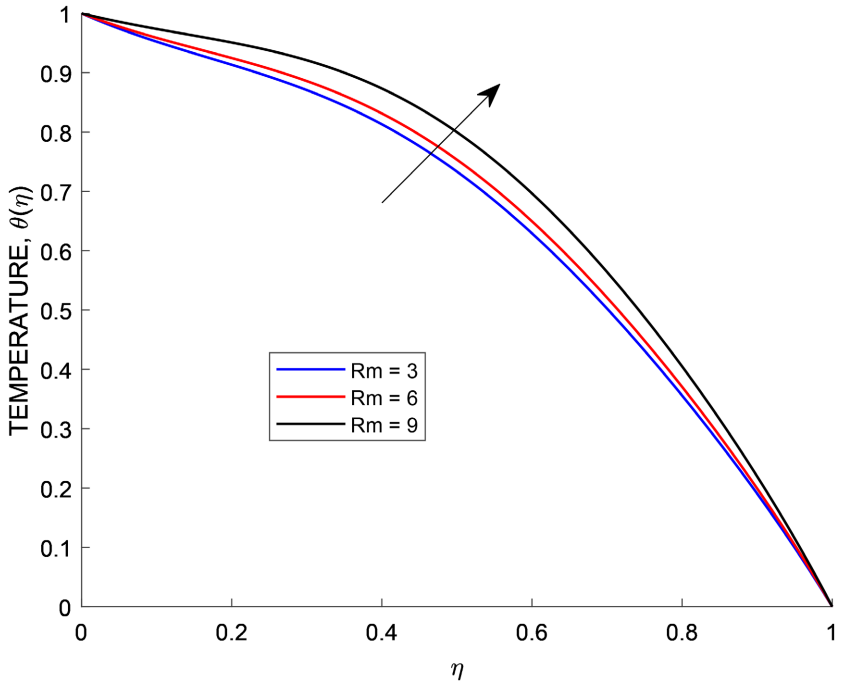

Figure 8. Temperature profiles with varying Reynold's magnetic number.

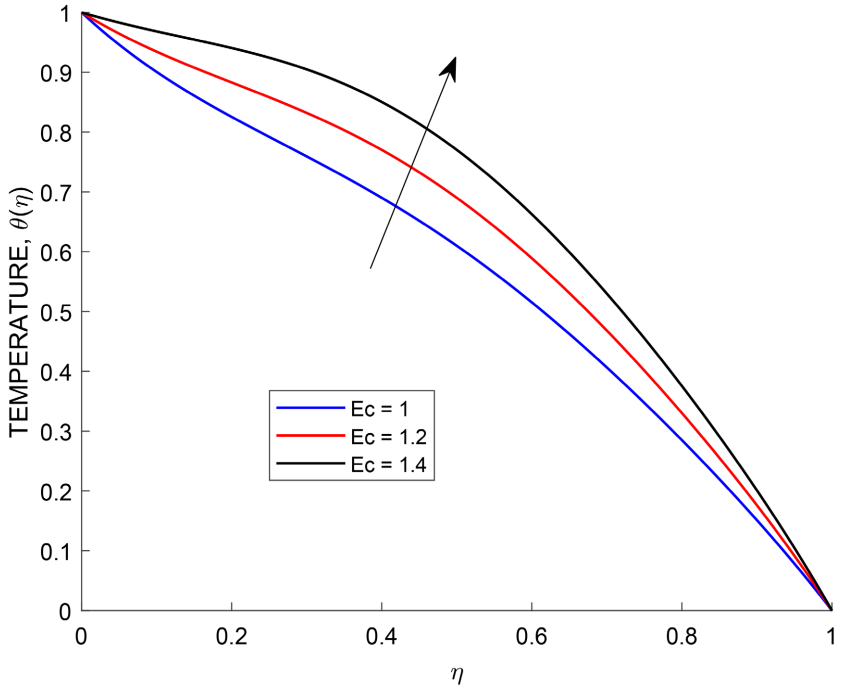

Figure 9. Temperature profiles with varying Eckert number.

in turns increases circulation pattern in the fluid and the rate of heat transfer. This enhance the heat transfer in the fluid and causes increase temperature.

From Figure 11, it is observed that magnetic induction profiles decreases as Reynold's magnetic number increases. Increasing Reynold's magnetic number reduces velocity which in turns reduced the magnetic diffusivity. This leads to a

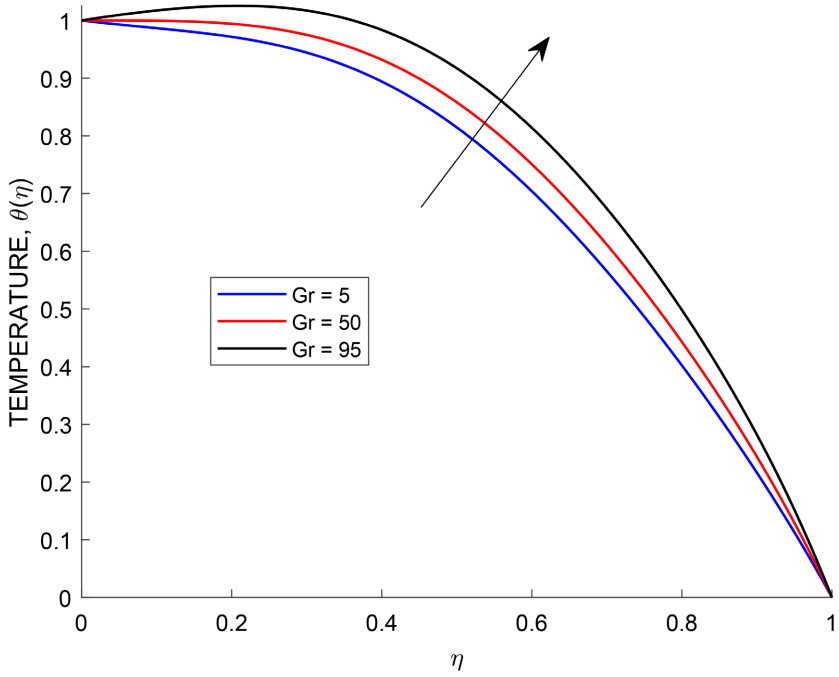

Figure 10. Temperature profiles with varying Thermal Grashof number.

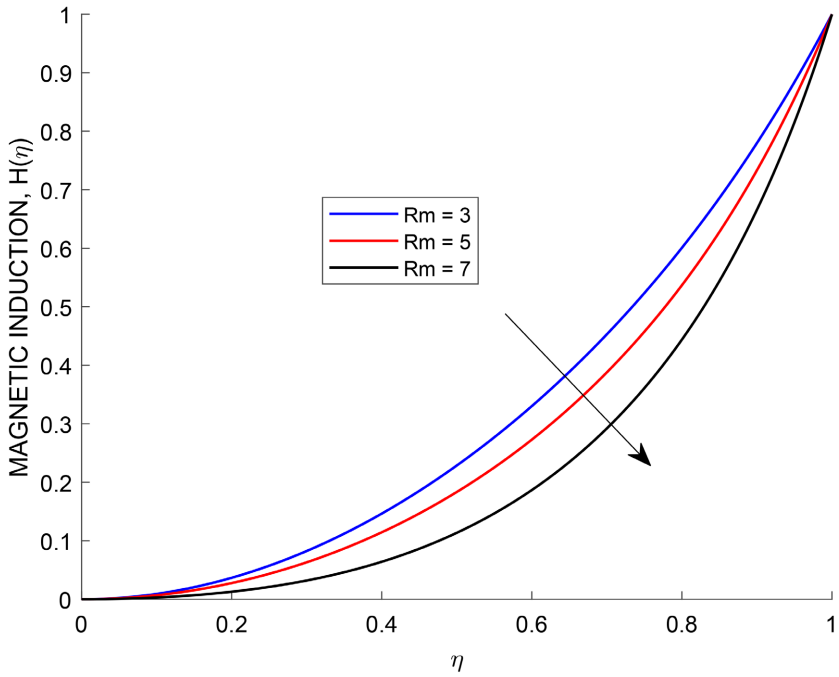

Figure 11. Magnetic induction profiles with varying Reynold's magnetic number.

decrease in induced magnetic field.

From Figure 12, it is observed that an increase in squeeze number increases the concentration profiles. An increase in the squeeze number causes an increase in the concentration of nanparticles of fluid between two plates due to increase in convective transport of the fluid than diffusive transport of the fluid. This increases the concentration of nanoparticles in the fluid because it reduces the dis-

tance between the fluid molecules and restricts their movement.

From Figure 13, it is observed that concentration profiles decreases with increase in Hartmann number. An increase in Hartmann number increases temperature in the fluid. Hence, this has the effect of causing a random transfer of nanoparticles in the fluid lowering mass leading to decrease in concentration in the fluid.

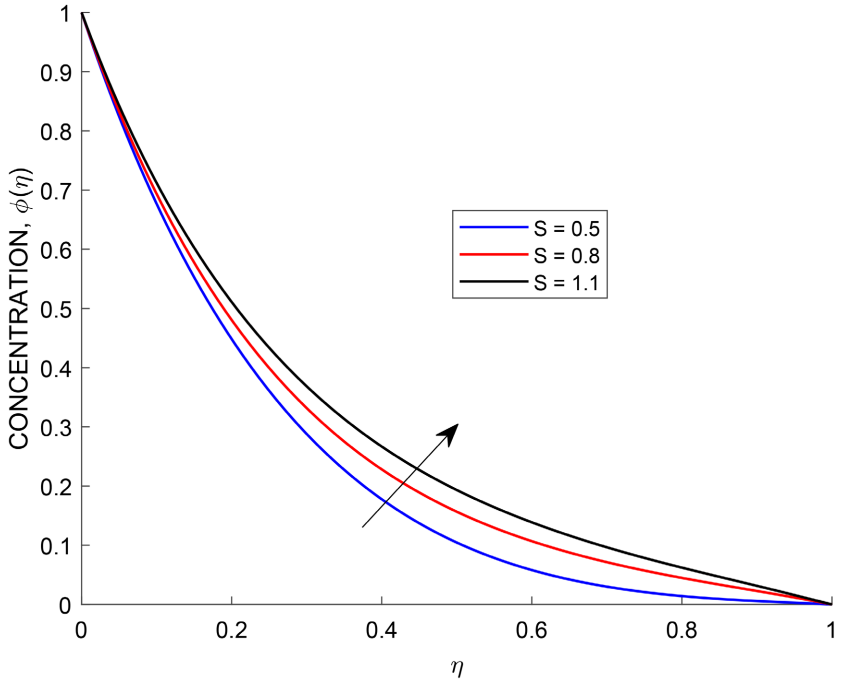

Figure 12. Concentration profiles with varying squeezing number.

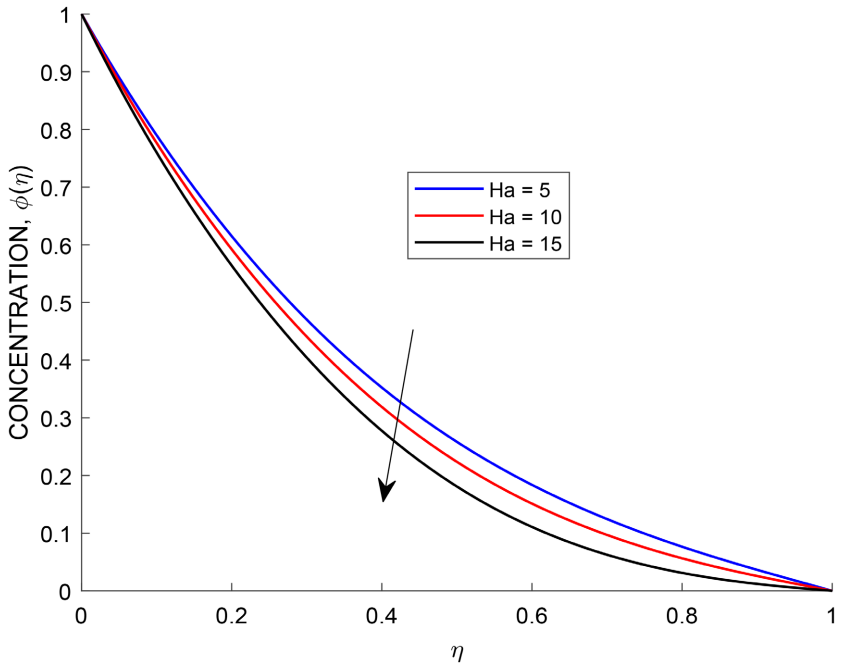

Figure 13. Concentration profiles with varying Hartmann number.

From Figure 14, it is observed that concentration profiles increases with increase in chemical reaction parameter-γ. An increase in chemical reaction parameter causes an increase in concentration profile because the nanoparticles are more likely to react with each other before they can diffuse away. This reaction process increases the concentration of nanoparticles in the fluid.

From Figure 15, it is observed that concentration profiles decreases with an increase in Joule heating number. Since increase in Joule heating increased

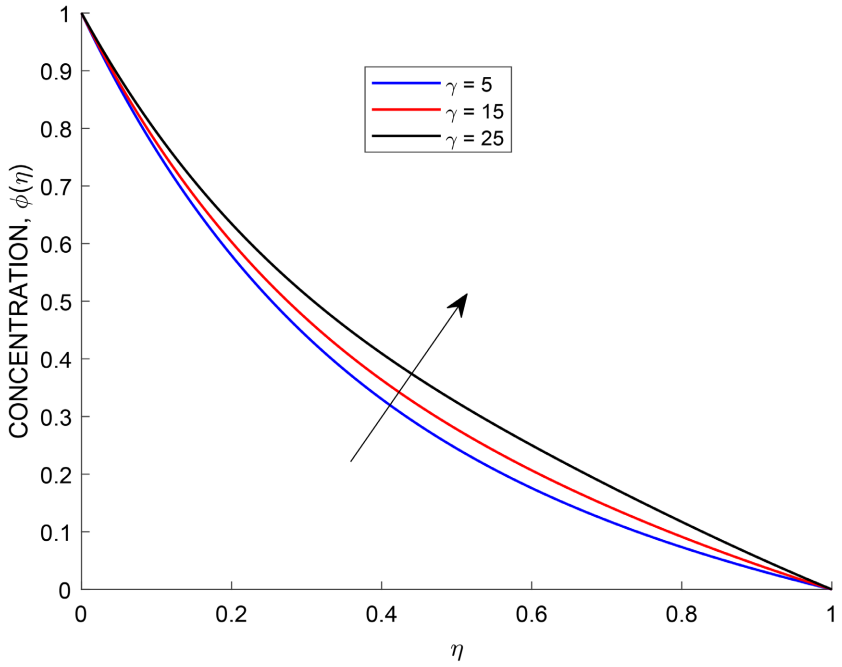

Figure 14. Concentration profiles with varying chemical reaction rate, γ.

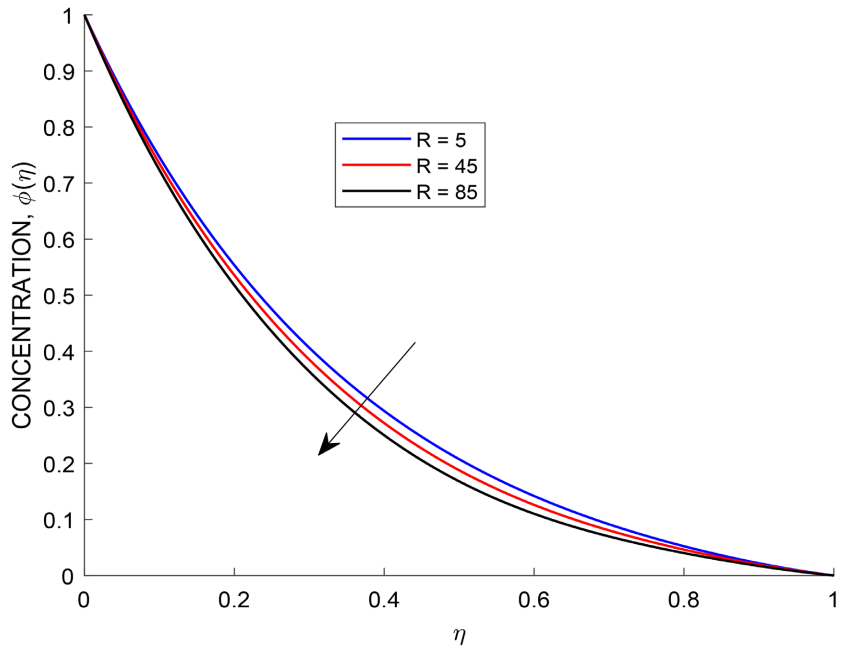

Figure 15. Concentration profiles with varying Joule heating number.

temperature of the fluid, then it has an accelerating effect of increasing diffusion rate in the fluid due to increase in temperature.

From Figure 16, it is observed that concentration profiles decrease with increase in Eckert number. Increase in Eckert number has the effect of increasing the temperature of the fluid. When the temperature of the fluid is increased, the diffusion of nanoparticles also increased. As a result, the concentration of the fluid decreases.

From Figure 17, it is observed that concentration profiles decreases with

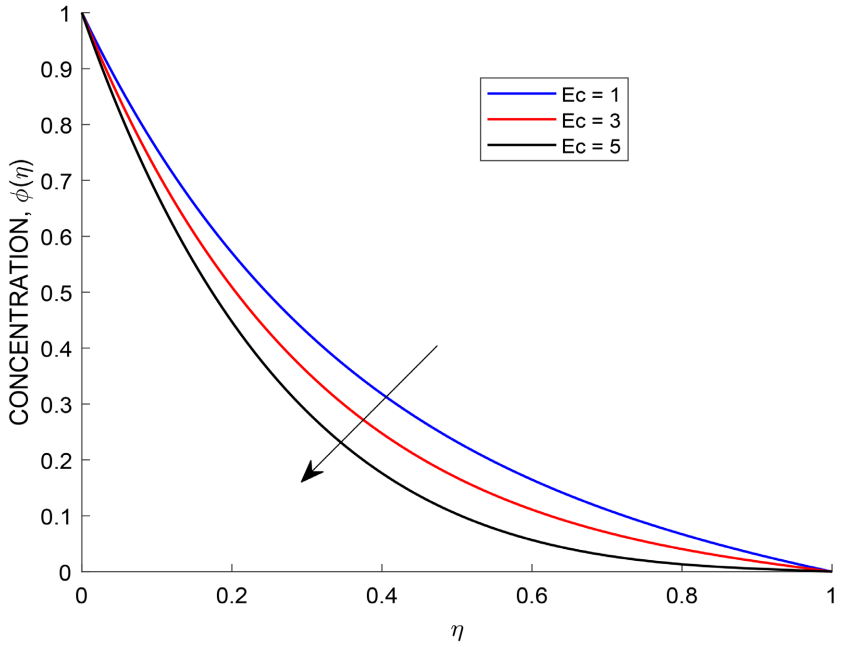

Figure 16. Concentration profiles with varying Eckert number.

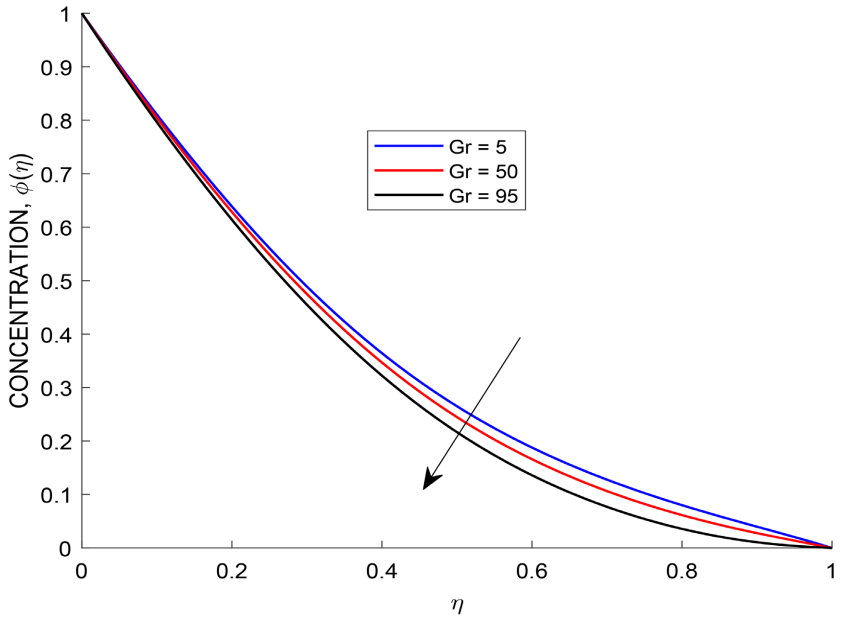

Figure 17. Concentration profiles with varying Thermal Grashof number.

increase in Thermal Grashof number. An increase in Thermal Grashof number increases buoyancy forces which enhance diffusion and reduced a boundary layer thickness. This leads to a decrease in concentration of nanoparticles in the fluid.

From Figure 18, it observed that concentration profiles decreases with increase in Schmidt number. Schmidt number is defined as a ratio of kinematic viscosity to mass diffusivity. When the Schmidt number increases, the mass diffusivity is reduced resulting into decrease in concentration of the fluid.

From Figure 19, it is observed that concentration profiles increases with an

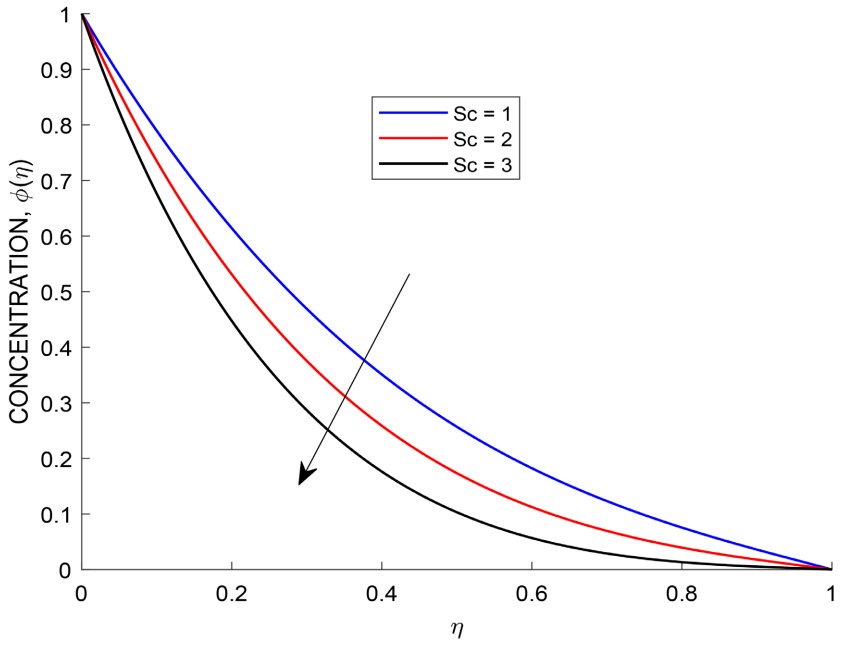

Figure 18. Concentration profiles with varying Schmidt number.

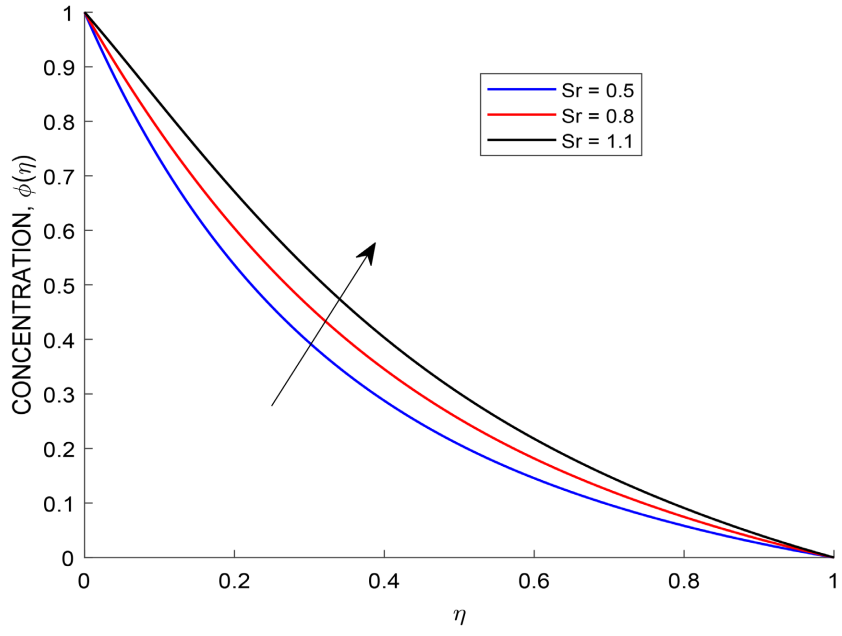

Figure 19. Concentration profiles with varying Soret number.

increase in Soret number. Under Soret effect, particles of different species have different thermal diffusivity. Hence, increasing the Soret number increases the temperature gradient and the thermal diffusivity difference between the particles leading to increase in concentration of the fluid.

6. Validation of Results

The validation of these results is done by comparison with results in the literature. The results are in agreement with results obtained by [17], which stated that velocity increases in the vicinity $0 \le \eta \le 1$ and that the velocity slows down with an increase in Hartmann number as shown in **Figure 20** and **Figure 21**.

7. Conclusions

In this study, Hydromagnetic Squeezing Nanofluid flow between two vertical

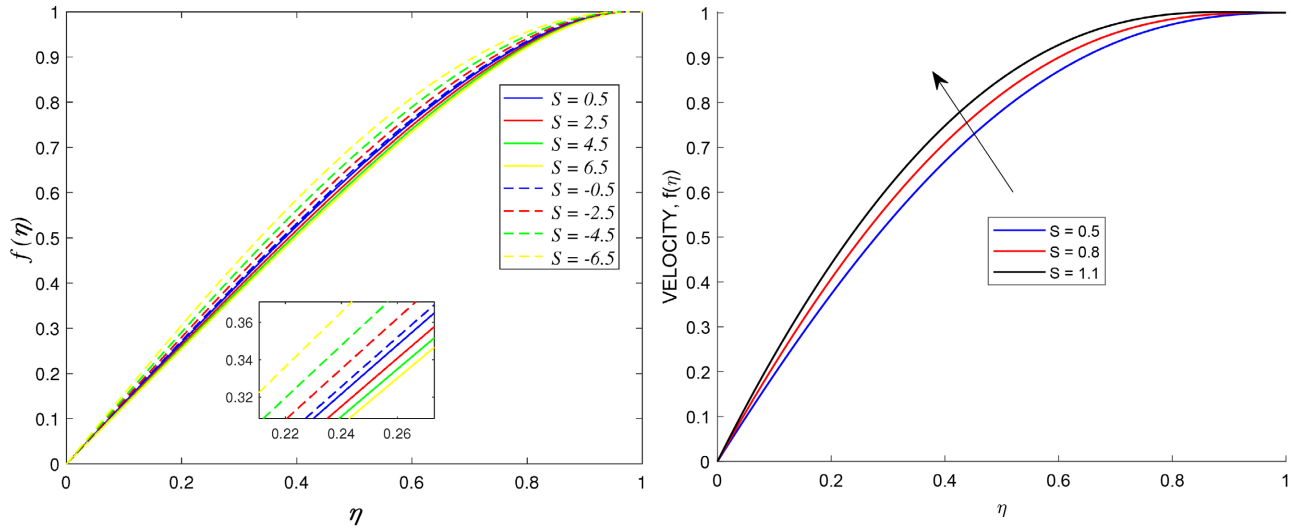

Figure 20. Velocity profiles with varying squeeze number.

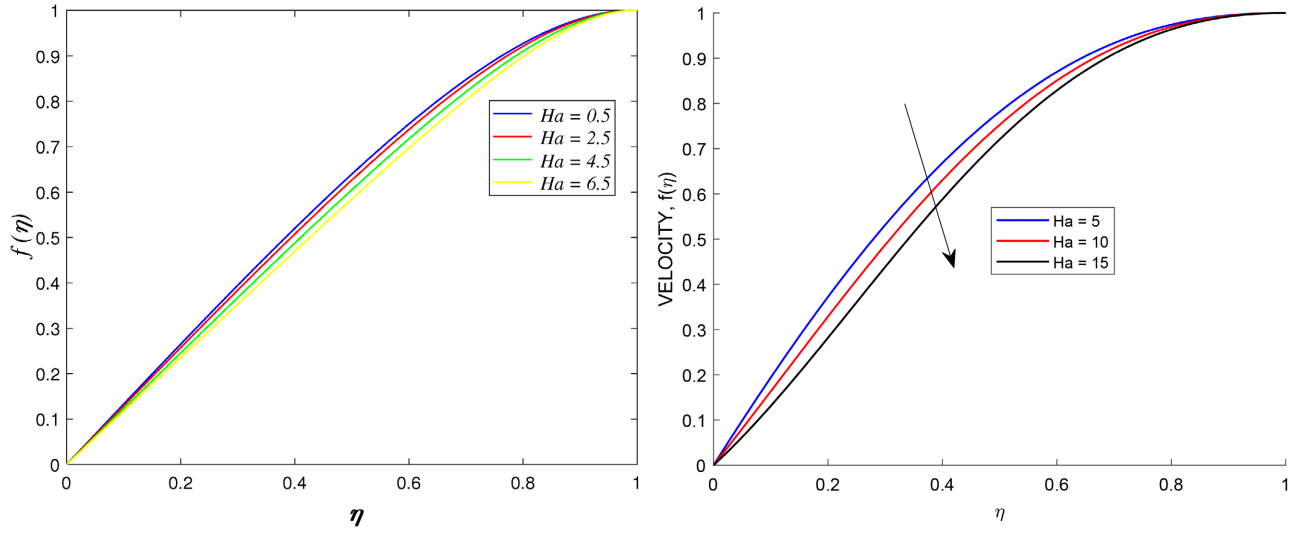

Figure 21. Velocity profiles with varying Hartmann number

plates in the presence of a chemical reaction has been investigated. The objectives were to determine the profiles for the velocity, temperature, concentration and induced magnetic field and determine the effects of various flow parameters discussed above. The governing equations were transformed into Ordinary Differential Equations (ODEs) using the similarity transformation and then converted into the system of the first ODES. The numerical solution is approximated using collocation method carried out using bvp4C in-build MATLAB function that displays the profiles graphically.

The characteristics observed in each profile were discussed and the overall conclusion was drawn as follows:

Increasing the squeeze number only boosts velocity and concentration while lowering temperature. Conversely, increasing the Hartmann number, Reynold's magnetic number, Eckert number and Thermal Grashof number generally increases temperature but decreases both velocity and concentration. Chemical reaction rate and Soret number solely elevate concentration while Schmidt number only reduces it.

Future research on nanofluid squeezing flow can explore the combined effects of multiple parameters, investigate the influence of different nanoparticle types and shapes and explore the implications of squeezing flow in various real-world applications. Additionally, developing more robust and efficient computational models will be crucial for further advancing the understanding of this complex phenomenon.

Data Availability

The data (MATLAB code) used to support the findings of this study are available from the corresponding author upon request. The data was generated by MATLAB software version R2021a (9.10.0.1602886).

Acknowledgments

The authors express gratitude to the African Union Commission on Education and the Pan African University Institute for Basic Sciences, Technology and Innovation (PAUSTI) for supporting this research project.

Conflicts of Interest

The authors declare no conflicts of interest regarding the publication of this paper.

References

[1] Alam, M.K., Bibi, K., Khan, A. and Noeiaghdam, S. (2404) Dufour and Soret Effect on Viscous Fluid Flow between Squeezing Plates under the Influence of Variable Magnetic Field. *Mathematics*, **9**, Article 2404. https://doi.org/10.3390/math9192404

[2] Atlas, M. (2021) Numerical Simulations of Squeezing Flow Problems in a Channel. Ph.D. Thesis, Capital University, Bexley.

[3] Choi, S.U.S. (1995) Developments and Applications of Non-Newtonian Flows. Amer-

ican Society of Mechanical Engineers, New York, 99-105.

[4] Khashi'ie, N.S., Waini, I., Arifin, N.Md. and Pop, I. (2021) Unsteady Squeezing Flow of Cu-Al_2O_3/Water Hybrid Nanofluid in a Horizontal Channel with Magnetic Field. *Scientific Reports*, **11**, Article No. 14128. https://doi.org/10.1038/s41598-021-93644-4

[5] Kotha, G., Kolipaula, V.R., Rao, M.V.S., Penki, S. and Chamkha, A.J. (2020) Internal Heat Generation on Bioconvection of an MHD Nanofluid Flow Due to Gyrotactic Microorganisms. *The European Physical Journal Plus*, **135**, Article No. 600. https://doi.org/10.1140/epjp/s13360-020-00606-2

[6] Lahmar, S., Kezzar, M., Eid, M.R. and Sari, M.R. (2020) Heat Transfer of Squeezing Unsteady Nanofluid Flow under the Effects of an Inclined Magnetic Field and Variable Thermal Conductivity. *Physica A*: *Statistical Mechanics and Its Applications*, **540**, Article ID: 123138. https://doi.org/10.1016/j.physa.2019.123138

[7] Sangeetha, P.S. and Nayak, S. (2022) Nanofluid Heat Transfer in Parallel Plates with Variable Magnetic Field. ArXiv: 2207.13485.

[8] Olabi, A.G., Wilberforce, T., Sayed, E.T., Elsaid, K., Atiqure Rahman, S.M. and Abdelkareem, M.A. (2021) Geometrical Effect Coupled with Nanofluid on Heat Transfer Enhancement in Heat Exchangers. *International Journal of Thermofluids*, **10**, Article ID: 100072. https://doi.org/10.1016/j.ijft.2021.100072

[9] Pandey, A.K. and Kumar, M. (2018) Squeezing Unsteady MHD Cu-Water Nanofluid Flow between Two Parallel Plates in Porous Medium with Suction/Injection. *Computational and Applied Mathematics Journal*, **4**, 31-42.

[10] Mohammad, R.-G., Oveis, P., Mofid, G.-B. and Domiri, G.D. (2017) The Effect of Variable Magnetic Field on Heat Transfer and Flow Analysis of Unsteady Squeezing Nanofluid Flow between Parallel Plates Using Galerkin Method. *Thermal Science*, **21**, 2057-2067. https://doi.org/10.2298/TSCI160524180R

[11] Shaheen, A., Imran, M., Waqas, H., Raza, M. and Rashid, S. (2023) Thermal Transport Analysis of Squeezing Hybrid Nanofluid Flow between Two Parallel Plates. *Advances in Mechanical Engineering*, **15**, 1-15. https://doi.org/10.1177/16878132221147453

[12] Sobamowo, M.G. and Akinshilo, A.T. (2018) On the Analysis of Squeezing Flow of Nanofluid between Two Parallel Plates under the Influence of Magnetic Field. *Alexandria Engineering Journal*, **57**, 1413-1423. https://doi.org/10.1016/j.aej.2017.07.001

[13] Su, X.H. and Yin, Y.X. (2019) Effects of an Inclined Magnetic Field on the Unsteady Squeezing Flow between Parallel Plates with Suction/Injection. *Journal of Magnetism and Magnetic Materials*, **484**, 266-271. https://doi.org/10.1016/j.jmmm.2019.04.041

[14] Umavathi, J.C., Patil, S.L., Mahanthesh, B. and Anwar Bég, O. (2021) Unsteady Squeezing Flow of a Magnetized Nano-Lubricant between Parallel Disks with Robin Boundary Conditions. *Proceedings of the Institution of Mechanical Engineers*, *Part N*: *Journal of Nanomaterials*, *Nanoengineering and Nanosystems*, **235**, 67-81. https://doi.org/10.1177/23977914211036562

[15] Jahangeer, I. (2020) Effects of an Inclined Magnetic Field on the Unsteady Squeezing Flow between Parallel Plates with Suction/Injection. Ph.D. Thesis, Capital University, Bexley.

[16] Hale, N. and Moore, D.R. (2006) A Sixth-Order Extension to the MATLAB Package bvp4c Software of J. Kierzenka and L. Shampine. Report No. 08/04.

[17] Noor, N.A.M., Shafie, S. and Admon, M.A. (2021) Slip Effects on MHD Squeezing Flow of Jeffrey Nanofluid in Horizontal Channel with Chemical Reaction. *Mathematics*, **9**, Article 1215. https://doi.org/10.3390/math9111215

Nomenclature

Symbol	Meaning
$\boldsymbol{q}$	Velocity Vector, ($m \cdot s^{-1}$)
$\boldsymbol{B}$	Magnetic induction strength, ($wb \cdot m^{-2}$)
$\boldsymbol{H}$	Magnetic field intensity, ($wb \cdot m^{-2}$)
$\boldsymbol{E}$	Electric field intensity, (V/m)
H_0	Applied inclined magnetic field vector, ($wb \cdot m^{-2}$)
H_y	Induced magnetic field along y direction, ($wb \cdot m^{-2}$)
H_x	Induced magnetic field along x direction, ($wb \cdot m^{-2}$)
x, y	Represent space coordinates, (m)
$\boldsymbol{J}$	Induction current density, ($A \cdot m^{-2}$)
p	pressure force, ($N \cdot m^{-2}$)
t	Time, (s)
a	Squeezing rate, (s^{-1})
L	Characteristics length, (m)
u, v	Represent velocity in x, y directions, ($m \cdot s^{-1}$)
k_{nf}	Nanofluid thermal conductivity, ($W \cdot m^{-1} \cdot K^{-1}$)
D_{nf}	Diffusive coefficient of nanofluid, ($m^2 \cdot s^{-1}$)
D_m	Mass diffusivity, ($m^2 \cdot s^{-1}$)
T_m	Mean temperature, (K)
K_t	Thermal diffusion ratio, ($m^2 \cdot s^{-1}$)
$\boldsymbol{F}$	Body forces, (N)
C_w	Concentration at the Wall, ($Mol \cdot m^{-3}$)
C_∞	Concentration at infinity, ($Mol \cdot m^{-3}$)
T_w	Wall temperature, (K)
T_∞	Temperature of the fluid at infinity, (K)
c_p	Specific heat capacity, ($J \cdot kg^{-1} \cdot K^{-1}$)
R_{nf}	Concentration reaction rate
k_r	Chemical reaction constant
S	Squeeze number
Pr	Prandtl number
Ha	Hartmann number
Ec	Eckert number
Sr	Soret number
Sc	Schmidt number
R	Joule heating number
R_m	Reyold's magnetic number
Gr	Grashof number for heat transfer
Gc	Grashof number for mass transfer

Greek Letters	Meaning
ρ_{nf}	Nanofluid density, (kg·m^{-3})
ρ_e	Charge density, (C)
α	An inclination angle, (rad)
θ	Dimensionless temperature
ϕ	Dimensionless concentration
η	Dimensionless similarity space variable
σ	Electrical conductivity, (Ω^{-1}·m^{-1})
μ_{nf}	Nanofluid coefficient of viscosity, kg·m^{-1} s)
μ_e	Magnetic permeability, (H·m^{-1})
Φ	Viscous dissipation function, (s^{-1})
ν_{nf}	Nanofluid kinematic viscosity, (m^2·s^{-1})
β_t	Volumetric thermal expansion, (K^{-1})
β_c	Volumetric concentration expansion, (kg·m^{-3})
δ	Length scale, (m)
γ	Chemical reaction parameter

Abbreviations

MHD	Magnetohyrodynamic
PDEs	Partial Differential Equations
ODEs	Ordinary Differential Equations
MATLAB	Matrix Laboratory